J. Phys. B: At. Mol. Opt. Phys. **43** (2010) 105204 (5pp) doi:10.1088/0953-4075/43/10/105204

Electron-impact double ionization of beryllium

M S Pindzola[1], C P Ballance[1], F Robicheaux[1] and J Colgan[2]

[1] Department of Physics, Auburn University, Auburn, AL, USA
[2] Theoretical Division, Los Alamos National Laboratory, Los Alamos, NM, USA

Received 1 March 2010, in final form 31 March 2010
Published 5 May 2010
Online at stacks.iop.org/JPhysB/43/105204

Abstract
Time-dependent close-coupling, *R*-matrix double pseudo-states and distorted-wave methods are used to calculate the electron-impact double ionization cross section for the $1s^2 2s^2$ ground state of the Be atom. At 1.5 times the double ionization threshold energy, the first two non-perturbative methods predict a cross section of approximately 1.0×10^{-18} cm^2 for the direct double ionization of the $2s^2$ subshell. At 15.0 times the double ionization threshold energy, the perturbative distorted-wave method predicts a cross section of approximately 2.0×10^{-18} cm^2 for the indirect single ionization of the $1s^2$ subshell followed by autoionization. Thus for the Be atom, the peak of the double ionization cross section is approximately two orders of magnitude smaller than the previously well-determined peak of the single ionization cross section.

(Some figures in this article are in colour only in the electronic version)

1. Introduction

The electron-impact double ionization of an atom at low energies results in three continuum electrons moving in the field of a charged core, that is the quantal Coulomb four-body problem. In recent years a non-perturbative method was developed based on the direct solution of the time-dependent Schrödinger equation for an incident electron scattering from an atom with two active target electrons. The time-dependent close-coupling (TDCC) method has been used to calculate total cross sections for the electron-impact double ionization of He [1, 2] and H^- [3] that are in good agreement with experiments [4, 5]. Pentuple energy and angle differential cross sections have also been calculated for the electron-impact double ionization of He [6] that are in only moderate agreement with the scaled shapes found in (e,3e) experiments [7].

Recently non-perturbative TDCC and perturbative distorted-wave methods were combined to calculate total cross sections for the electron-impact double ionization of Mg [8]. At low energies the non-perturbative direct double ionization cross sections for the $3s^2$ subshell were found to be in good agreement with experiment, and at higher energies the perturbative indirect double ionization cross sections coming from single ionization of the $2s^2$ and $2p^6$ inner subshells followed by autoionization were also found to be in good agreement with experiment [9, 10]. For the Mg atom, the peak of the double ionization cross section is around 2.5×10^{-17} cm^2, while the peak of the single ionization cross section is around 4.0×10^{-16} cm^2 [11].

In a previous study [12], we examined the electron-impact single ionization of Be using the non-perturbative TDCC and R-matrix pseudo-states (RMPS) methods. Collision processes involving Be are important since it has been chosen for first-wall plasma facing components in ITER [13]. In this paper, we examine the electron-impact double ionization of Be. At low energies we calculate the direct double ionization cross sections for the $2s^2$ subshell using the non-perturbative TDCC method and a newly developed R-matrix double pseudo-states (RMDPS) method. At higher energies we calculate the indirect double ionization cross sections coming from the single ionization of the $1s^2$ inner subshell followed by autoionization using a perturbative distorted-wave method. We hope our theoretical predictions will stimulate an experiment to measure the total cross section for the electron-impact double ionization of Be.

The remainder of this paper is organized as follows. In section 2, we review the perturbative distorted-wave and TDCC methods, and present the new RMDPS method. In section 3, we apply the various methods to the calculation of the electron-impact double ionization cross section of Be over a wide energy range. In section 4, we conclude with a

summary and an outlook for future work. Unless otherwise stated, all quantities are given in atomic units.

2. Theory

2.1. Configuration-average distorted-wave method

The configuration-average distorted-wave (CADW) expression for the electron-impact single ionization cross section of the $(n_t l_t)^{w_t}$ subshell of any atom is given by [14]

$$\sigma_{\rm single} = \frac{16 w_t}{k_i^3} \int_0^E \frac{{\rm d}\epsilon_e}{k_e k_f} \sum_{l_i,l_e,l_f} (2l_i+1)(2l_e+1) \times (2l_f+1)\mathcal{P}(n_t l_t, k_i l_i, k_e l_e, k_f l_f), \quad (1)$$

where the linear momenta (k_i, k_e, k_f) and the angular momenta (l_i, l_e, l_f) quantum numbers correspond to the incoming, ejected and outgoing electrons, respectively. The total energy $E = \epsilon_i - I = \epsilon_e + \epsilon_f$, where I is the subshell ionization energy and $\epsilon = \frac{k^2}{2}$. The first-order perturbation theory expression for the scattering probability $\mathcal{P}(n_t l_t, k_i l_i, k_e l_e, k_f l_f)$ is given in terms of standard $3j$ and $6j$ symbols and radial Slater integrals [14]. The bound radial orbitals, $P_{nl}(r)$, needed to evaluate the Slater integrals are calculated using a Hartree–Fock atomic structure code [15]. The continuum radial orbitals, $P_{kl}(r)$, needed to evaluate the Slater integrals are calculated by solving the radial Schrödinger equation using a Hartree with local exchange potential. The incident and scattered electron continuum radial orbitals are evaluated in a $\rm V_{if}^N$ potential ($N = 4$ for Be), while the ejected continuum radial orbital is calculated in a $\rm V_e^{N-1}$ potential [16]. Alternatively, all the continuum radial orbitals are calculated in a $\rm V_{ief}^{N-1}$ potential [17]. For an N electron neutral atom, the continuum solutions in a $\rm V^N$ potential see an asymptotic charge of zero, while the continuum solutions in a $\rm V^{N-1}$ potential see an asymptotic charge of one. The continuum normalization for all the distorted waves is one times a sine function.

2.2. Time-dependent close-coupling method on a 2D lattice

For electron-impact single ionization of the ns^2 subshell of an atom with one active electron, the TDCC-2D equations for each LS symmetry are given by [18]

$$\mathrm{i}\frac{\partial P_{l_1 l_2}^{LS}(r_1,r_2,t)}{\partial t} = T_{l_1 l_2}(r_1,r_2) P_{l_1 l_2}^{LS}(r_1,r_2,t) + \sum_{l_1',l_2'} V_{l_1 l_2, l_1' l_2'}^{L}(r_1,r_2) P_{l_1' l_2'}^{LS}(r_1,r_2,t), \quad (2)$$

where $P_{l_1 l_2}^{LS}(r_1,r_2,t)$ is a two-electron radial wavefunction, $T_{l_1 l_2}(r_1,r_2)$ is a two-fold sum over one-electron kinetic, nuclear and atomic core operators, and $V_{l_1 l_2, l_1' l_2'}^{L}(r_1,r_2)$ is a two-electron repulsion operator.

The initial condition for the solution of the TDCC-2D equations is given by

$$P_{l_1 l_2}^{LS}(r_1,r_2,t=0) = P_{ns}(r_1) G_{k_0 l_0}(r_2) \delta_{l_1,0} \delta_{l_2,l_0}, \quad (3)$$

where $P_{ns}(r)$ is a bound radial orbital for the active electron, and $G_{k_0 l_0}(r)$ is a Gaussian radial wavepacket with energy $\frac{k_0^2}{2}$.

Following the time propagation of the TDCC-2D equations, the total single ionization cross section is given by

$$\sigma_{\rm single} = \frac{\pi}{2k_0^2} \int_0^\infty {\rm d}k_1 \int_0^\infty {\rm d}k_2 \sum_{L,S} (2L+1)(2S+1) \times \sum_{l_1,l_2} \left| P_{l_1 l_2}^{LS}(k_1 l_1, k_2 l_2) \right|^2, \quad (4)$$

where $P_{l_1 l_2}^{LS}(k_1 l_1, k_2 l_2)$ is a two-electron momentum space wavefunction obtained by projection of the time-evolved coordinate space wavefunctions onto fully anti-symmetric products of two box-normalized continuum orbitals.

2.3. Time-dependent close-coupling method on a 3D lattice

For electron-impact single and double ionization of the ns^2 subshell of an atom with two active electrons, the TDCC-3D equations for each $\mathcal{LS}$ symmetry are given by [18]

$$\mathrm{i}\frac{\partial P_{l_1 l_2 L l_3}^{\mathcal{LS}}(r_1,r_2,r_3,t)}{\partial t} = T_{l_1 l_2 l_3}(r_1,r_2,r_3) P_{l_1 l_2 L l_3}^{\mathcal{LS}}(r_1,r_2,r_3,t) + \sum_{l_1',l_2',L',l_3'} \sum_{i<j}^{3} V_{l_1 l_2 L l_3, l_1' l_2' L' l_3'}^{\mathcal{L}}(r_i,r_j) P_{l_1' l_2' L' l_3'}^{\mathcal{LS}}(r_1,r_2,r_3,t), \quad (5)$$

where $P_{l_1 l_2 L l_3}^{\mathcal{LS}}(r_1,r_2,r_3,t)$ is a three-electron radial wavefunction, $T_{l_1 l_2 l_3}(r_1,r_2,r_3)$ is a three-fold sum over one-electron kinetic, nuclear and atomic core operators, and $V_{l_1 l_2 L l_3, l_1' l_2' L' l_3'}^{\mathcal{L}}(r_i,r_j)$ is a two-electron repulsion operator.

The initial condition for the solution of the TDCC-3D equations is given by

$$P_{l_1 l_2 L l_3}^{\mathcal{LS}}(r_1,r_2,r_3,t=0) = \sum_{l} \bar{P}_{ll}(r_1,r_2,\tau\to\infty) G_{k_0 l_0}(r_3) \delta_{l_1,l} \delta_{l_2,l} \delta_{L,0} \delta_{l_3,l_0}, \quad (6)$$

where the two-electron radial wavefunctions $\bar{P}_{ll}(r_1,r_2,\tau)$ are obtained by solution of a set of TDCC-2D equations for the relaxation of a two-electron atom in imaginary time (τ). Following the time propagation of the TDCC-3D equations, the total single ionization cross section is given by

$$\sigma_{\rm single} = \frac{\pi}{2k_0^2} \int_0^\infty {\rm d}k_2 \int_0^\infty {\rm d}k_3 \sum_{\mathcal{L},\mathcal{S}} (2\mathcal{L}+1)(2\mathcal{S}+1) \times \sum_{L,S} \sum_{l_2,l_3} \left| P_{l_2 L S l_3}^{\mathcal{LS}}(ns, k_2 l_2, k_3 l_3) \right|^2, \quad (7)$$

where $P_{l_2 L S l_3}^{\mathcal{LS}}(ns, k_2 l_2, k_3 l_3)$ is a three-electron momentum space wavefunction obtained by projection of the time-evolved coordinate space wavefunctions onto fully anti-symmetric products of a bound orbital and two box-normalized continuum orbitals. The total double ionization cross section is given by

$$\sigma_{\rm double} = \frac{\pi}{2k_0^2} \int_0^\infty {\rm d}k_1 \int_0^\infty {\rm d}k_2 \int_0^\infty {\rm d}k_3 \sum_{\mathcal{L},\mathcal{S}} (2\mathcal{L}+1)(2\mathcal{S}+1) \times \sum_{L,S} \sum_{l_1,l_2,l_3} \left| P_{l_1 l_2 L S l_3}^{\mathcal{LS}}(k_1 l_1, k_2 l_2, k_3 l_3) \right|^2, \quad (8)$$

where $P_{l_1 l_2 L S l_3}^{\mathcal{LS}}(k_1 l_1, k_2 l_2, k_3 l_3)$ is a three-electron momentum space wavefunction found by projection of the time-evolved coordinate space wavefunctions onto fully anti-symmetric products of three box-normalized continuum orbitals.

2.4. R-matrix double pseudo-states method

The RMPS method was developed [19, 20] to calculate cross sections for the electron-impact excitation and ionization of atoms and their ions. Electron-impact single ionization cross sections for the $2s^2$ subshell of Be were previously calculated using the RMPS method [12]. This required a single pseudo-state expansion of the form $1s^2 2s\bar{n}\bar{l}$ where the 1s and 2s are spectroscopic orbitals and the nl correspond to associated Laguerre polynomials over a user-defined range of the principal quantum number n and the orbital angular momentum l. When considering single ionization from the metastable configuration $1s^2 2s2p$, we added the $1s^2 2p\bar{n}\bar{l}$ pseudo-state expansion to allow for the ionization of either the 2s or 2p orbitals. A natural extension of this method to model three electrons in the continuum is to attach complete pseudo-state expansions to configurations that already contain a single pseudo-orbital of the form $1s^2\bar{n}\bar{l}\bar{n}'\bar{l}'$ with the previously mentioned $1s^2 2l\bar{n}\bar{l}$ expansions.

In our implementation of the RMDPS method, the basis used to represent the $(N + 1)$-electron continuum was made orthogonal to the pseudo-orbitals using a method developed by Gorczyca and Badnell [20]. The scattering calculation was performed with a set of parallel R-matrix programs [21, 22], which are extensively modified versions of the serial RMATRIX I programs [23]. Inside the R-matrix box, the total wavefunction for a given LS symmetry is expanded in basis states given by

$$\Psi_k^{N+1} = A \sum_{i,j} a_{ijk} \psi_i^{N+1} \frac{u_{ij}(r_{N+1})}{r_{N+1}} + \sum_i b_{ik} \chi_i^{N+1}, \qquad (9)$$

where A is an antisymmetrization operator, ψ_i^{N+1} are the channel functions obtained by coupling N-electron target states with the angular and spin functions of the scattered electron, $u_{ij}(r)$ are the radial continuum basis functions and χ_i^{N+1} are bound functions which ensure completeness of the total wavefunction. For the ground state of Be, the configurations corresponding to the N-electron component of the channel functions ψ_i^{N+1} will have the form

$$\psi_i^N = 1s^2\bar{n}\bar{l}\bar{n}'\bar{l}'. \qquad (10)$$

The coefficients a_{ijk} and b_{ik} are determined by diagonalization of the total $(N + 1)$-electron Hamiltonian.

Outside the R-matrix box, the total wavefunction for a given LS symmetry is expanded in basis states given by

$$\Psi_k^{N+1} = \sum_i \psi_i^{N+1} \frac{v_i(r_{N+1})}{r_{N+1}}. \qquad (11)$$

The radial continuum functions, $v_i(r)$, are solutions to the coupled differential equations given by

$$T_i(r)v_i(r) + V_{ij}(r)v_j(r) = 0\,, \qquad (12)$$

where $T_i(r)$ is a kinetic and nuclear energy operator and $V_{ij}(r)$ is an asymptotic coupling operator. Above the double ionization threshold, the coupled differential equations are solved on a coarse energy mesh. The inner and outer solutions are matched at the edge of the R-matrix box, and the K-matrix is extracted. The electron-impact double ionization is simply the sum of excitation cross sections from the ground state and those terms associated with the $1s^2\bar{n}\bar{l}\bar{n}'\bar{l}'$ configurations above the double ionization threshold. We note that care must be taken to omit contributions from the ground state to the terms associated with the $1s^2 2s\bar{n}\bar{l}$ and $1s^2 2p\bar{n}\bar{l}$ configurations, corresponding to single ionization.

Table 1. Partial cross sections in Mb for the electron-impact single ionization of the Be atom at an incident energy of 40 eV (1.0 Mb = 1.0×10^{-18} cm^2).

Partial wave L	CADW V_{if}^N/V_e^{N-1}	CADW V_{ief}^{N-1}	TDCC-2D V_{pp1}	TDCC-2D V_{pp2}	TDCC-3D V_{pp1}
0	7.9	5.9	5.2	4.1	2.9
1	26.8	21.4	12.8	13.1	10.4
2	33.8	31.3	23.8	25.3	21.7
3	30.0	28.4	27.3	26.4	22.3
4	30.5	25.6	31.7	27.8	22.1
5	31.2	27.0	35.8	29.5	21.4
6	28.4	27.5	–	–	–
7	23.4	25.2	–	–	–
8	18.0	21.1	–	–	–
9	13.3	16.4	–	–	–

3. Results

As a check on the TDCC-3D method, electron-impact single ionization cross sections for the $1s^2 2s^2$ ground state of the Be atom were calculated at an incident energy of 40 eV. Electron-impact single ionization cross sections for the $2s^2$ subshell of Be were calculated using the CADW method described in section 2.1. The CADW partial cross sections for the V_{if}^N/V_e^{N-1} and V_{ief}^N choices for the scattering potentials are presented in the second and third columns of table 1. Electron-impact single ionization cross sections for the $2s^2$ subshell of Be were calculated using the TDCC-2D method described in section 2.1 on a 192×192 point mesh with a uniform mesh spacing of $\Delta r = 0.20$. The TDCC-2D partial cross sections for a V_{pp1} pseudo-potential used in previous e + Be collision calculations [12] and for a V_{pp2} pseudo-potential generated for molecular calculations [24] are presented in the fourth and fifth columns of table 1. Electron-impact single ionization cross sections for the $2s^2$ subshell of Be were calculated using the TDCC-3D method described in section 2.3 on a $192 \times 192 \times 192$ point mesh with a uniform mesh spacing of $\Delta r = 0.20$. The TDCC-3D partial cross sections for a V_{pp1} pseudo-potential are presented in the sixth column of table 1. In general, the trends for the partial cross sections as a function of partial wave are in reasonable agreement for all five calculations. The non-perturbative TDCC results are generally smaller than the perturbative CADW results for the low L partial cross sections, as has been found in almost all other electron–atom collision calculations [18]. The TDCC-2D results are found to be insensitive to the choice of core pseudo-potential. Finally, the TDCC-2D and TDCC-3D results are found to be in reasonable agreement, although the TDCC-3D results are on average about 25% smaller for each partial cross section.

Non-perturbative RMDPS calculations were then carried out for electron-impact double ionization of the $2s^2$ subshell

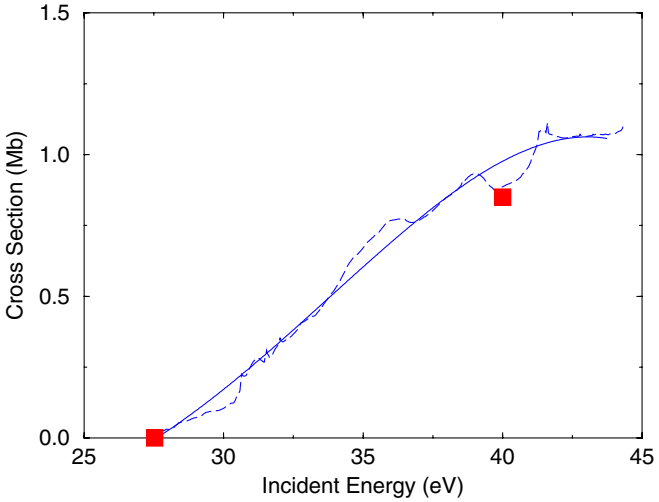

Figure 1. Electron-impact double ionization of Be. Solid squares: TDCC calculations for direct double ionization of the $2s^2$ subshell; solid line: RMDPS fitted calculations for direct double ionization of the $2s^2$ subshell; dashed line: RMDPS raw calculations for direct double ionization of the $2s^2$ subshell (1.0 Mb = 1.0×10^{-18} cm^2).

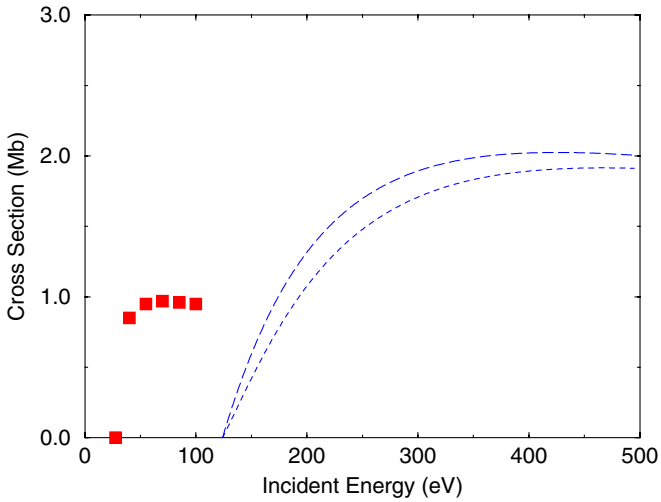

Figure 2. Electron-impact double ionization of Be. Solid squares: TDCC calculations for direct double ionization of the $2s^2$ subshell; long dashed line: CADW calculations using V_{ief}^{N-1} potentials for indirect ionization–autoionization of the $1s^2$ subshell; short dashed line: CADW calculations using V_{if}^{N}/V_{e}^{N-1} potentials for indirect ionization–autoionization of the $1s^2$ subshell (1.0 Mb = 1.0×10^{-18} cm^2).

of ground state Be. For the RMDPS calculations, the *R*-matrix box has a radius of 83.0 Bohr radii and we employ 58 basis orbitals to represent the $(N+1)$-electron continuum per angular momentum. This should be sufficient to span the incident electron energy range from the double ionization threshold to 45.0 eV. We included all 683 LS terms arising from $1s^2 2s\bar{n}\bar{l}$, $1s^2 2p\bar{n}\bar{l}$, $1s^2 3\bar{s}\bar{n}\bar{l}$, $1s^2 3\bar{p}\bar{n}\bar{l}$, and $1s^2 3\bar{d}\bar{n}\bar{l}$ in both the configuration interaction description of the target and the close-coupling expansion of the scattering calculation. The pseudo-orbitals range from $n = 3$ to 14 in principal quantum number and $l = 0$ to 4 in orbital angular momentum for each of the above expansions. In total, our scattering model included 48 scattering partial waves from $L = 0$ to 11 and resulted in Hamiltonian matrices as large as 92 000 × 92 000. For this particular model the double ionization cross section is simply the summation of cross sections from the ground state to those terms arising from only the $1s^2 3\bar{l}\bar{n}'\bar{l}'$ configurations. Total cross sections for electron-impact double ionization are shown in figure 1. A simple analytic formula was used to fit the RMDPS results and thus smooth out the unphysical oscillations due to the presence of continuum pseudo-state resonances.

Non-perturbative TDCC-3D calculations were then carried out for electron-impact double ionization of the $2s^2$ subshell of ground state Be. Using a 192 × 192 point mesh with a uniform mesh spacing of $\Delta r = 0.20$ and the core pseudo-potential V_{pp1} used in previous single ionization calculations [12], relaxation of the TDCC-2D equations in imaginary time yielded the $\bar{P}_{ll}(r_1, r_2, \tau \to \infty)$ radial wavefunctions of equation (6) with a double ionization potential of 27.7 eV, compared to the experimental value of 27.5 eV [25]. Using a 192 × 192 × 192 point mesh with a uniform mesh spacing of $\Delta r = 0.20$, the TDCC-3D equations were propagated in real time for $\mathcal{L} = 0$–5 $\mathcal{S} = \frac{1}{2}$ total symmetries and for five incident energies ranging from 40 eV to 100 eV. The partial cross sections were extrapolated to higher $\mathcal{L}$ using a nonlinear angular momentum fitting expression given by

$$\sigma(\mathcal{L}) = c_1 \mathcal{L}^{c_2} \, e^{-\frac{2I_d}{E}\mathcal{L}}, \tag{13}$$

where I_d is the double ionization potential, E is the incident energy, and c_1, c_2 are fitting coefficients. Total cross sections for electron-impact double ionization are shown in figures 1 and 2. As seen in figure 1, the non-perturbative RMDPS and TDCC-3D methods are in good agreement for the direct double ionization cross section of the $2s^2$ subshell of Be at an incident electron energy of 40 eV.

Finally, perturbative CADW calculations were carried out for the electron-impact single ionization of the $1s^2$ subshell of ground state Be. For ionization of a tightly bound inner subshell, the CADW method should be reasonably accurate. We assume the branching ratio for autoionization of the $1s2s^2$ state of Be^+ to be 1. Total cross sections for the indirect ionization–autoionization of Be are shown in figure 2 from the 1s inner subshell ionization threshold of 124 eV to 500 eV. The CADW calculations using the V_{ief}^{N-1} potentials are found to give cross sections slightly larger than the CADW calculations using V_{if}^{N}/V_{e}^{N-1} potentials, opposite to what is found in table 1 for the single ionization of the $2s^2$ subshell. As seen in figure 2, the non-perturbative TDCC-3D cross sections for the direct double ionization of Be peak at 1.0 Mb around 70 eV, while the perturbative CADW cross sections for the indirect double ionization of Be peak at 2.0 Mb close to 450 eV.

4. Summary

In conclusion, the TDCC, RMDPS and distorted-wave methods were used to calculate the electron-impact double ionization of the beryllium atom. For the first time, the *R*-matrix method was applied to an electron–atom collision

process involving three continuum electrons. At an incident energy of 40 eV, the non-perturbative RMDPS and TDCC-3D methods were found to be in good agreement for the magnitude of the direct double ionization cross section of the outer subshell of Be. Further TDCC-3D calculations found that the direct double ionization cross section for Be peaks at 1.0 Mb around 70 eV. The perturbative CADW method was then used to calculate indirect ionization–autoionization cross sections for the inner subshell of Be. The indirect double ionization cross section for Be was found to peak at 2.0 Mb around 450 eV. Thus for the Be atom, the magnitude of the double ionization cross section is approximately two orders of magnitude smaller than the single ionization cross section [12], as compared to a factor of 16 for Mg [8, 11]. In addition, the ratio of indirect to direct double ionization of a factor of 2.0 for Be compares to a factor of 8.0 for Mg. The 1s inner subshell ionization cross sections for Be are much smaller than the 2s and 2p inner subshell ionization cross sections for Mg.

We hope that the current calculations will stimulate an experimental study of the electron-impact double ionization of Be. In the future, we plan to apply the non-perturbative RMDPS and TDCC-3D methods to study direct double ionization processes in electron collisions with singly charged atomic ions.

Acknowledgments

This work was supported in part by grants from the US Department of Energy. Computational work was carried out at the National Energy Research Scientific Computing Center in Oakland, CA, and at the National Institute for Computational Sciences in Oak Ridge, TN.

References

[1] Pindzola M S, Robicheaux F, Colgan J, Witthoeft M C and Ludlow J A 2004 *Phys. Rev.* A **70** 032705
[2] Pindzola M S, Robicheaux F and Colgan J 2007 *Phys. Rev.* A **76** 024704
[3] Pindzola M S, Robicheaux F and Colgan J 2006 *J. Phys. B: At. Mol. Opt. Phys.* **39** L127
[4] Shah M B, Elliott D S, McCallion P and Gilbody H B 1988 *J. Phys. B: At. Mol. Opt. Phys.* **21** 2751
[5] Yu D J, Rachafi S, Jureta J and Defrance P 1992 *J. Phys. B: At. Mol. Opt. Phys.* **25** 4593
[6] Pindzola M S, Robicheaux F and Colgan J 2008 *J. Phys. B: At. Mol. Opt. Phys.* **41** 235202
[7] Durr M, Dorn A, Ullrich J, Cao S P, Czasch A, Kheifets A S, Gotz J R and Briggs J S 2007 *Phys. Rev. Lett.* **98** 193201
[8] Pindzola M S, Ludlow J A, Robicheaux F, Colgan J and Griffin D C 2009 *J. Phys. B: At. Mol. Opt. Phys.* **42** 215204
[9] McCallion P, Shah M B and Gilbody H B 1992 *J. Phys. B: At. Mol. Opt. Phys.* **25** 1051
[10] Boivin R F and Srivastava S K 1998 *J. Phys. B: At. Mol. Opt. Phys.* **31** 2381
[11] Ludlow J A, Ballance C P, Loch S D, Pindzola M S and Griffin D C 2009 *Phys. Rev.* A **79** 032715
[12] Colgan J, Loch S D, Pindzola M S, Ballance C P and Griffin D C 2003 *Phys. Rev.* A **68** 032712
[13] Hawryluk R J *et al* 2009 *Nucl. Fusion* **49** 065012
[14] Pindzola M S, Griffin D C and Bottcher C 1986 *Atomic Processes in Electron–ion and Ion–Ion Collisions* (NATO ASI B vol 145) p 75
[15] Cowan R D 1981 *The Theory of Atomic Structure and Spectra* (Berkeley, CA: University of California Press)
[16] Younger S M 1981 *Phys. Rev.* A **24** 1278
[17] Botero J and Macek J H 1991 *J. Phys. B: At. Mol. Opt. Phys.* **24** L405
[18] Pindzola M S *et al* 2007 *J. Phys. B: At. Mol. Opt. Phys.* **40** R39
[19] Bartschat K, Hudson E T, Scott M P, Burke P G and Burke V M 1996 *J. Phys. B: At. Mol. Opt. Phys.* **29** 115
[20] Gorczyca T W and Badnell N R 1997 *J. Phys. B: At. Mol. Opt. Phys.* **30** 3897
[21] Mitnik D M, Pindzola M S, Griffin D C and Badnell N R 1999 *J. Phys. B: At. Mol. Opt. Phys.* **32** L479
[22] Ballance C P and Griffin D C 2004 *J. Phys. B: At. Mol. Opt. Phys.* **37** 2943
[23] Berrington K A, Eissner W B and Norrington P H 1995 *Comput. Phys. Commun.* **92** 290
[24] Stevens W J, Basch H and Krauss M 1984 *J. Chem. Phys.* **81** 6026
[25] http://physics.nist.gov/PhysRefData